ChemElectroChem

Articles
doi.org/10.1002/celc.202101283

Chemistry Europe
European Chemical Societies Publishing

www.chemelectrochem.org

Electrodeposition of Cu onto Au(111) from Deep Eutectic Solvents: Molar Ratio of Salt and Hydrogen Bond Donor

Tanja Geng,[a] Sven J. Zeller,[a, b, c] Ludwig A. Kibler,[a] Maximilian U. Ceblin,*[a] and Timo Jacob*[a, b, c]

The electrodeposition of copper onto Au(111) from Deep Eutectic Solvents (DESs) type III has been studied by cyclic voltammetry. Investigations were carried out with mixtures of choline chloride (ChCl) and ethylene glycol (EG) or trifluoroacetamide (TFA). The eutectic compositions and temperatures were determined by differential scanning calorimetry (DSC). For the ChCl/EG DES, a eutectic ratio of 16:84 (ChCl:EG) was found instead of the previously reported ratio of 33:67. The electrodeposition of copper was studied for electrolytes with different ratios of ChCl to hydrogen bond donor (HBD) to resolve the influence of the composition on the deposition behavior. Both CuCl and $CuCl_2$ were used as Cu salts. Underpotential deposition (UPD) is followed by bulk deposition with the diffusion rate of Cu species being dependent on the ratio of ChCl to HBD. With $CuCl_2$, both Cu^+ and Cu^{2+} species are reduced and deposited, whereby the two-electron reduction is more dominant with higher chloride content and presence of EG. However, the properties of the Cu electrodeposition do not result from the freezing-point depression of the DESs, but from the high concentration of ions.

Introduction

Recently, there has been an increasing interest in developing non-aqueous electrolytes for application in batteries[1–3] and electroplating.[4–6] In particular, the electrodeposition of non-noble metals such as chromium, aluminum, magnesium, and sodium is the subject of numerous investigations.[5–8] The electrodeposition of these metals is impossible or at least very difficult from aqueous electrolytes and often, *e.g.* in the case of chromium, toxic and environmentally harmful deposition baths are used.[9,10] A promising and rather new class of electrolytes are deep eutectic solvents (DESs). DESs typically consist of a hydrogen bond donor in combination with an organic or inorganic salt, which is referred to as DES type III and DES type IV, respectively.[11,12] For the eutectic composition, they typically represent liquids at room temperature due to freezing-point depression. As the two components are usually inexpensive and can be purified separately, DESs are suitable for large-scale applications and in technologies where high purity is required.[13,14] Both the salt and the HBD can be chosen to be non-toxic for obtaining an environmentally compatible electrolyte. Further advantages are the rather low viscosity compared to ionic liquids, the high electric conductivity, and a wide electrochemical stability window.[13] The HBD can act as an additive to conveniently tune the deposition kinetics, as well as the surface morphology of the deposited metal.[15] So far, metals such as copper and silver, but also more reactive metals including zinc, nickel, chromium, and aluminum have been deposited from DESs on different substrates.[13,15–17]

Since copper deposition is of great importance both in industry and in fundamental research, it has already been investigated rather extensively.[18–20] These investigations serve as a starting point for the present study, as they provide a fundamental understanding of copper deposition in aqueous and non-aqueous systems and can be used as reference. Copper deposition on an Au(111) single crystal electrode is therefore an ideal model system for fundamental investigations with this new class of electrolytes.

Several important aspects of copper electrodeposition from DESs type III are known already. Copper and copper composites were deposited from $CuCl_2$ in ChCl/urea and ChCl/EG DES on platinum.[16] It was found that the complexation of copper ions and therefore the deposition kinetics and thermodynamics are different compared to aqueous electrolytes. This phenomenon is mainly attributed to the high chloride concentration in the DESs. Cu deposition was also investigated in a ChCl/urea DES with $CuCl_2$ on a glassy carbon electrode and compared with the behavior of highly concentrated aqueous chloride solutions.[17,21] These systems behave similarly and show a high stabilization of Cu^+ species by chloride. With the same DES, underpotential deposition of copper on Au(*hkl*) single crystals has been studied.[22] The kinetics of the electron transfer reaction between Cu^+ and Cu^{2+} in a DES of ChCl/EG on platinum electrodes has been the subject of several studies.[23–25] In all

[a] T. Geng, S. J. Zeller, Dr. L. A. Kibler, Dr. M. U. Ceblin, Prof. Dr. T. Jacob
Institute of Electrochemistry
Ulm University
Albert-Einstein-Allee 47, 89081 Ulm, Germany
E-mail: maximilian.ceblin@uni-ulm.de
        timo.jacob@uni-ulm.de
[b] S. J. Zeller, Prof. Dr. T. Jacob
Helmholtz-Institute Ulm (HIU) for Electrochemical Energy Storage
Helmholtzstr. 11, 89081 Ulm, Germany
[c] S. J. Zeller, Prof. Dr. T. Jacob
Karlsruhe Institute of Technology (KIT)
P.O. Box 3640, 76021 Karlsruhe, Germany

cases, the diffusion of Cu ions in solution is slower than in aqueous systems due to the higher viscosity of the DESs.

Despite the extensive research in the field of DESs performed over the last years, there is little knowledge about their thermal behavior.[26,27] This holds especially true for the impact of composition on the freezing point and the resulting freezing-point depression. So far, there has been no detailed investigation on whether or how the molar ratio of salt and HBD influences the deposition behavior. Therefore, in the present study we address the questions of whether freezing-point depression and eutectic ratio influence the electrodeposition process, and if DESs show unique behavior as electrolytes with high ion concentration. We will show that the electrolyte composition itself, independently of the eutectic ratio, influences the conductivity as well as the complexes present in the electrolyte, and thus the electrochemical behavior.

In this study, we investigate the thermal and electrochemical characteristics of different DESs systematically as a function of composition. For this purpose, we choose two different DESs type III: The ChCl/EG system, which is one of the most widely studied, and the ChCl/TFA DES, which is selected because TFA can be easily purified by sublimation as it does not decompose upon melting, which is in contrast to the behavior of urea. First, DSC is applied to obtain phase diagrams and to determine the eutectic ratios and eutectic temperatures of the different DESs. The subsequent electrochemical deposition of copper onto Au(111) serves as a model reaction. Cu^+ or Cu^{2+} species are added to the DES mixtures. An Au(111) single crystal is employed to study the initial stages of the Cu electrodeposition from mixtures of different compositions by cyclic voltammetry.

Results and Discussion

Thermal characterization

Various mixtures of choline chloride and ethylene glycol of different ratios were analyzed by DSC. The heating curves of each sample are shown in Figure 1. In all cases, multiple exothermic peaks in the range between $-90\,°C$ and $-40\,°C$, corresponding to recrystallization, are observed. During fast cooling, the samples are forming amorphous glasses and when reheated slowly, the mixtures first crystallize before melting. A slow heating rate of $0.2\,°C\,min^{-1}$ was chosen to separate recrystallization and melting so that both the melting temperature and the melting enthalpy can reliably be determined.

The first endothermic process occurs at the same temperature for all samples under study. Here, the eutectic melts, thus representing the eutectic temperature. All mixtures except the eutectic one exhibit a subsequent broad endothermic effect. The end of this second melting process is visible as an endothermic peak with subsequent sharp return to the baseline for the mixtures with more EG. For the samples with more ChCl, the effect exhibits only low heat flow and is therefore indicated by an arrow for better visibility. The temperature and the shape of this endothermic peak strongly depend on the molar ratio
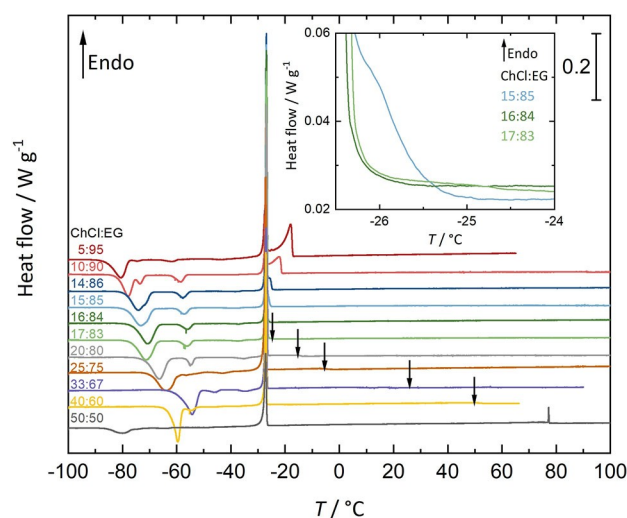

Figure 1. DSC curves of ChCl/EG mixtures of different compositions were obtained with a heating rate of $0.2\,°C\,min^{-1}$ from -100 to $100\,°C$. Endothermic (signal up) and exothermic peaks (signal down) correspond to melting and crystallization, respectively. For better readability, the thermograms are shifted against each other. The arrows indicate the second melting peak of the corresponding thermograms. Inset: Curve sections in the ratios 15:85, 16:84, and 17:83 (ChCl:EG). The 16:84 sample corresponds to the eutectic and thus shows only one melting point.

between salt and HBD. As it changes with the amount of excess component, it is associated with the melting of the non-eutectic crystals which then dissolve into the melt. The only curve with only the first and not the second melting point corresponds to the sample with eutectic composition, *i.e.* there is no component in excess. To identify this curve in a better way, the inset in Figure 1 shows the part of the DSC curves after the first melting point of three mixtures. The ChCl/EG sample with a ratio of 15:85 exhibits a clear second melting peak at $-26.0\,°C$. For the 17:83 mixture, there is a second melting process occurring until $-24.7\,°C$, just visible as being slightly above the baseline. However, the curve of the ChCl/EG 16:84 sample returns directly to the baseline after the melting of the eutectic is complete. Thus, the eutectic ratio of the ChCl/EG DES is shown to be at 16:84.

The 50:50 sample with a high excess of ChCl shows a characteristic feature regarding the second melting peak. After the first melting peak, as expected, the curve rises continuously, but the second melting peak appears as a spike at $77.1\,°C$. Pure ChCl exhibits a similar peak starting at $76.6\,°C$. A corresponding phase transition occurring at $73–80\,°C$ from the orthorhombic to a partially disordered cubic form is known.[28] Besides, similar behavior has been found for the well-known ChCl/urea DES, where all samples with $x(ChCl)\geq0.45$ show a transition at $78.5\,°C$.[27] At this temperature, the α-phase of the remaining solid excess choline chloride transforms into β-ChCl. This process occurs independently of the HBD present in the system.

To obtain a phase diagram from the DSC curves, each curve is analyzed separately. This is illustrated in Figure 2 for ChCl/EG in the ratio of 10:90 as an example. First, the onset temperature of the eutectic melting peak is determined. It is defined as the intersection point of a sigmoidal baseline connecting the curves
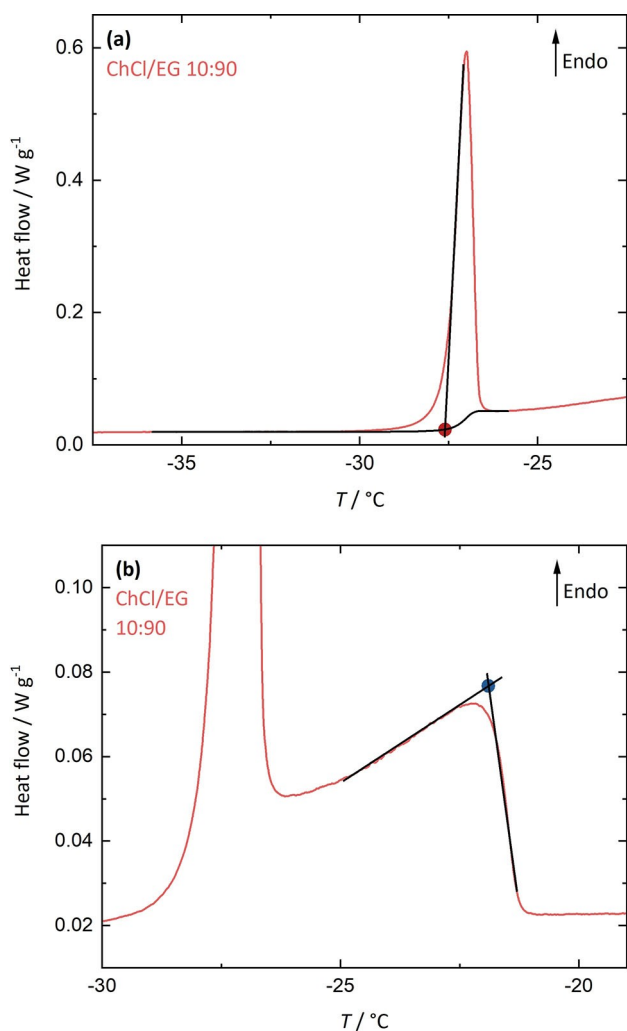
ChemElectroChem

Articles
doi.org/10.1002/celc.202101283

**Chemistry
Europe**

European Chemical
Societies Publishing

Figure 2. DSC curve sections of ChCl/EG with ratio 10:90 at a heating rate of 0.2 °C min^{-1}. A Baseline (in a) and construction lines (a and b) were added to the thermograms to determine the solidus (a, red dot) and liquidus (b, blue dot) temperature.

Figure 3. a) Phase diagram of the ChCl/EG DES as a function of the molar fraction of choline chloride. The solidus line (red) was determined by a linear fit with a slope of zero and the liquidus line (blue) by a two-part piecewise linear fit. b) Tammann plot for the melting enthalpy of the eutectic transition fitted by a two-part piecewise linear fit to determine the maximum.

before and after the peak with a tangent to the inflection point of the ascending part of the curve (Figure 2a).[29] This yields the solidus temperature of the binary mixture. To determine the liquidus temperature, corresponding to the end of the melting of the excess component, the second melting event is examined (Figure 2b). The intersection point of the two tangents obtained from the thermal flux after the solidus peak and the line of return to the baseline results in the desired temperature.

For each ratio, *i.e.* for each DSC curve, the respective solidus and liquidus temperatures are plotted against the mole fraction x(ChCl). This yields the phase diagram of the ChCl/EG DES (Figure 3a). The eutectic temperature, which corresponds to that of the solidus line, is obtained by linear regression with a slope of zero and amounts to -27.6 ± 0.2 °C. Above this temperature, the eutectic mixture is purely liquid. The liquidus line is determined by a two-part piecewise linear fit resulting in a minimum at a ratio of 16.5:83.5. This corresponds nicely to the DSC curve of the 16:84 mixture, which has a single and
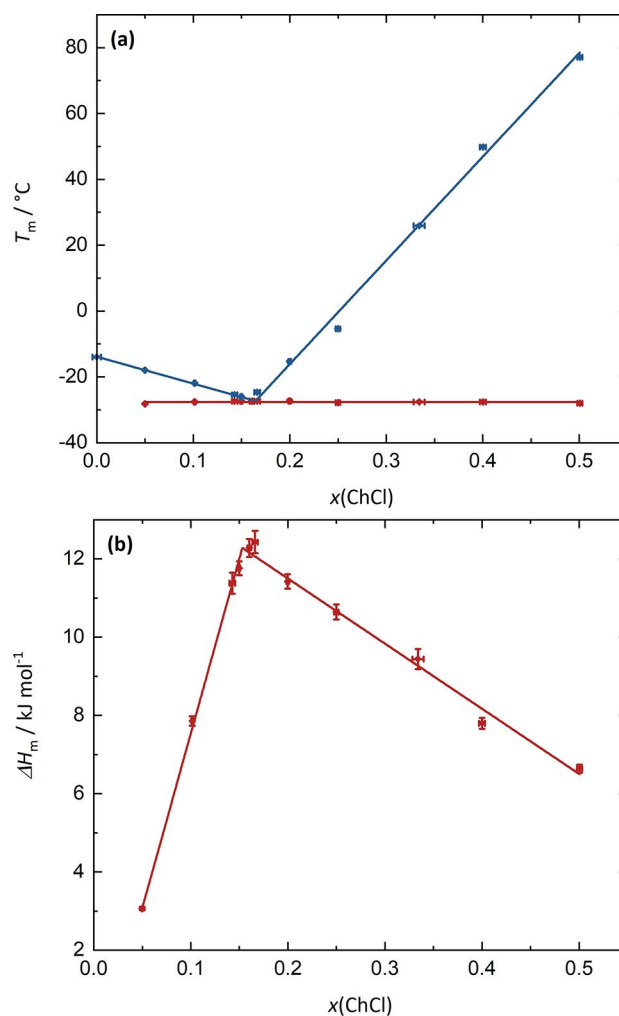
therefore the lowest melting point. Besides, the enthalpies of melting of the eutectic crystals have been determined by integration of the thermal flux over time. These melting enthalpies are shown as a function of the composition in a Tammann plot (Figure 3b). Since the eutectic mixture is melting at the eutectic point, there is a maximum in the melting enthalpy for this composition. With more excess component that melts at higher temperatures, the melting enthalpy at the eutectic temperature decreases linearly. The maximum is calculated by a two-part piecewise linear fit at a ratio of 15.3:84.7 with a melting enthalpy of 12.3 ± 0.3 kJ mol^{-1}. These results are in good agreement with the eutectic ratio (16:84) and enthalpy (12.3 ± 0.3 kJ mol^{-1} and accordingly 165 ± 2 J g^{-1}) determined from the DSC curves themselves. However, those findings are quite surprising, as the eutectic ratio does not coincide with the one normally used (33:67).[13] Our results are compared to literature at the end of this section.

ChemElectroChem

Articles
doi.org/10.1002/celc.202101283

**Chemistry
Europe**
European Chemical
Societies Publishing

To better understand the influence of the HBD on the thermal properties, a different DES consisting of ChCl and TFA has been analyzed by DSC as well. The same procedure was applied, so Figure 4a shows the heating step ($0.2\,°C\,min^{-1}$) of ChCl/TFA mixtures in different ratios. The DSC curves have a similar shape as for the ChCl/EG DES. First, the samples recrystallize between $-50\,°C$ and $-10\,°C$, seen as exothermic peaks. The first endothermic melting peak occurs at a constant temperature for all mixtures and thus corresponds to the eutectic temperature. The second melting peak strongly depends on the composition and its temperature increases on moving away from the eutectic. The eutectic mixture showing only the first melting point has a ratio of 31:69. This means that one molecule of choline chloride interacts with more than two (2.2) molecules of trifluoroacetamide. Interestingly, this is not an integer, as was also observed for ChCl/EG.

Following the same procedure as for the ChCl/EG DES (Figure S1), the phase diagram is obtained (Figure 4b) with a
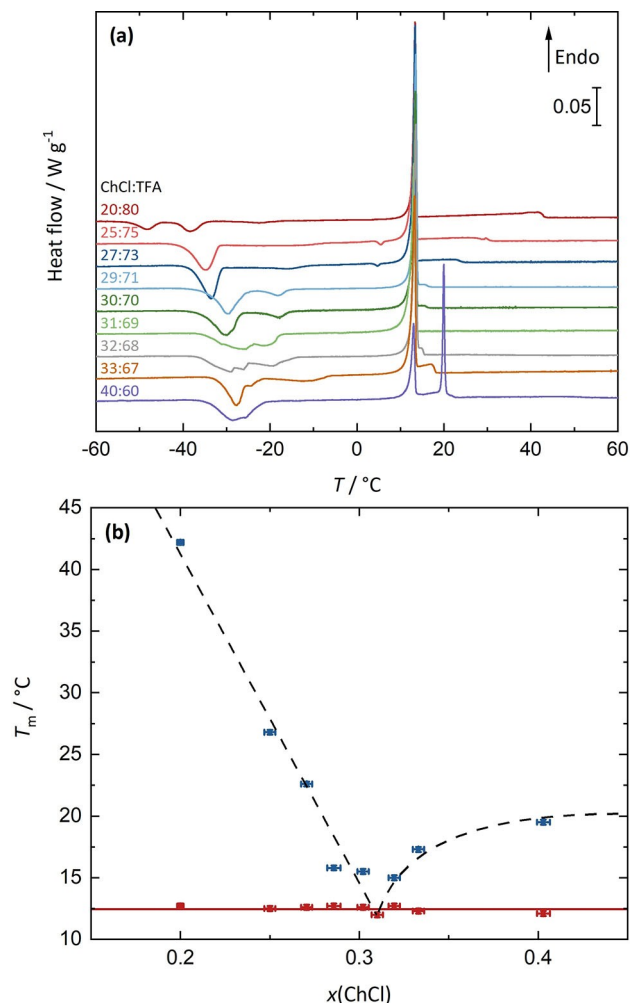
eutectic temperature (red line) of $12.5\pm0.2\,°C$. The liquidus line (dashed black line) starts at the eutectic point rising first strongly and then more slowly as the respective excess component increases. In this case, it exhibits a rather round shape instead of a linear slope in both directions. The melting enthalpies of the eutectic are again depicted in a Tammann plot as a function of composition (Figure S2). The maximum of the ChCl/TFA DES is located at a ratio of 30.8:69.2 with a corresponding melting enthalpy of $10.9\pm0.2\,kJ\,mol^{-1}$. These results fit well with the eutectic ratio (31:69) and melting enthalpy ($10.6\pm0.2\,kJ\,mol^{-1}$ and accordingly $87.4\pm0.9\,J\,g^{-1}$) obtained directly from the DSC curves.

The thermal properties of the ChCl/TFA DES have previously been investigated using its freezing point.[30] For excess of TFA ($x(ChCl)<0.29$), a white precipitate was observed at room temperature. For this reason, the ratio of 29:71 with a freezing point of $-45\,°C$ was assumed to be the eutectic ratio. The agreement with our result despite the low number of mixtures analyzed seems by sheer chance. The low freezing point indicates that severe supercooling has occurred since the eutectic temperature determined during heating is significantly higher.

For the ChCl/EG DES, it has been claimed that the eutectic ratio would be 33:67.[13,14] This DES in this specific ratio has first been used by Abbott et al.[31–33], but it is not evident from these publications why exactly the 1:2 ratio should be the eutectic one. Investigating the freezing point of various ChCl/EG mixtures, the lowest freezing point has been found for $x(ChCl)=0.33$ and 0.34 at $-66\,°C$.[30,34] However, the heating mode would be more suitable to determine a phase diagram, especially if organic substances are involved.[29] Apparently, supercooling caused a major drawback in this case, which led to a strong distortion of the results. This is also evident from the very low freezing point compared to the melting temperature: The second melting process of the ChCl/EG 33:67 mixture ends only at $25.9\,°C$ (Figure 1). If a sample of this DES is stored for a longer time at room temperature, it may even freeze. However, this presupposes that pure chemicals were used, otherwise the melting-point depression would be larger so that the second melting point would drop below room temperature. Another study examined the phase diagram of this mixture by the oil bad method (melting temperature is the optically last solid disappearance), a melting point device, and by DSC, depending on the composition. In this case, a minimum melting temperature was found at $x(ChCl)=0.38$ with $-32\,°C$.[35] The difference to our results could be due to the higher heating rate ($2\,°C\,min^{-1}$ compared to $0.2\,°C\,min^{-1}$) in the DSC measurements and the smaller accuracy of the other methods. The slower the heating rate, the better is the separation of the eutectic melting peak to that of excess component and therefore, the more accurate is the determination of the melting points.[29] This can influence the obtained phase diagram drastically. However, a recent study found the lowest melting point of the ChCl/EG mixture for $x(ChCl)=0.17$ (ChCl/EG 1:5) at $-67\,°C$.[36] This ratio is very similar to our results. Unfortunately, no experimental details have been given.

Figure 4. a) DSC curves of ChCl/TFA mixtures of different compositions obtained with a heating rate of $0.2\,°C\,min^{-1}$ from -100 to $100\,°C$. Only the relevant part is shown. For better readability, the thermograms were shifted against each other. b) Phase diagram of the ChCl/TFA DES as a function of the mole fraction of ChCl. The solidus line (red) was determined by a linear fit with a slope of zero and the dashed black line indicates the course of the liquidus line.

ChemElectroChem

Articles
doi.org/10.1002/celc.202101283

**Chemistry
Europe**
European Chemical
Societies Publishing

When mixing ChCl/EG in the ratio of 33:67, it is supposed that one molecule of ChCl is neighbored by two EG molecules. With a eutectic ratio of 16:84, we find that one ChCl molecule is surrounded by more than five (5.3) molecules of EG, which is more than double the amount reported previously. This has obviously a huge impact on the intermolecular interactions and therefore on the physical properties of this DES, such as the melting point. But it also influences the electrochemical properties and kinetics of metal deposition, as will be shown below.

For the ChCl/urea DES, which is frequently used, the eutectic ratio has already been determined by various groups. First, the freezing point has been analyzed resulting in a eutectic ratio of 33:67.[11] In this case, the same ratio was found when examining the melting process by DSC and additional methods.[26,27,37,38] To the best of our knowledge, melting enthalpies of eutectic mixtures have so far only been reported for the ChCl/urea DES. In this case, a melting enthalpy of 8.1 kJ mol^{-1} has been obtained,[37] compared to 12.3 ± 0.3 kJ mol^{-1} for ChCl/EG and 10.9 ± 0.2 kJ mol^{-1} for ChCl/TFA. Regarding the eutectic ratio, we suspect that the ChCl/urea and ChCl/EG DES were assumed to have an identical eutectic ratio. It appears that the influence of the HBD on the thermal properties has been underestimated. The importance of the HBD is also apparent by the differing melting-point depression of the two DESs under study. In the case of the ChCl/EG DES, the melting-point depression (difference between the melting point of the pure HBD and the eutectic temperature) amounts to 14.6 °C compared to the melting point of pure EG. With 60.9 °C compared to the melting of TFA, the melting-point depression of the ChCl/TFA DES is more than four times higher. The question arises whether differences between various hydrogen bond donors, for example in electrodeposition behavior, may have been observed in some publications only due to differing molar ratios between salt and HBD.

Electrochemical characterization of Au(111) in ChCl/EG

For the electrochemical measurements, the DESs were prepared in their eutectic as well as in other ratios. The electrochemical behavior of the ChCl/EG DES in its eutectic ratio (16:84) is studied thoroughly and compared to that of ChCl/EG (33:67). The latter was chosen because it is commonly employed.[13,14]

Figure 5a shows cyclic voltammograms for an Au(111) single crystal electrode in contact with both mixtures over the whole electrochemical stability window. In both electrolytes, several adsorption and desorption processes take place between 0.3 and 0.8 V$_{Cu}$. The eutectic mixture exhibits slightly higher current densities. These might be related to the significantly different chloride concentrations, which amount to 1.9 mol L^{-1} in the 16:84 and 3.4 mol L^{-1} in the 33:67 mixture. Since surface oxidation of gold starts positive of 0.8 V$_{Cu}$, a potential limit of 0.9 V$_{Cu}$ was chosen. At potentials negative of 0.3 V$_{Cu}$, a purely capacitive double-layer region can be identified. The negative potential limit is dictated by the HBD, in this case by EG. At about -0.7 V$_{Cu}$, EG starts to decompose, presumably by polymerization. If the fraction in EG is larger (blue curve),
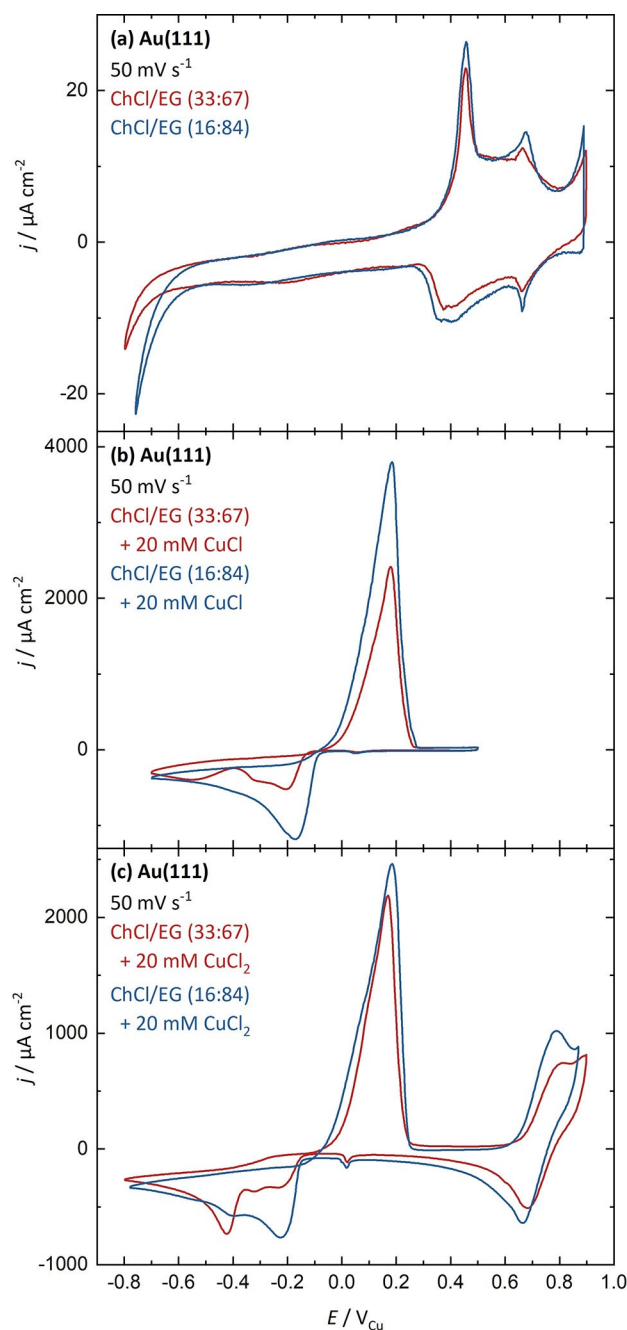

Figure 5. Cyclic voltammograms of Au(111) in choline chloride/ethylene glycol mixtures in a ratio of 33:67 (red) and 16:84 (blue) (a), with 20 mM CuCl (b) or 20 mM CuCl$_2$ (c) at a scan rate of 50 mV s^{-1}.

decomposition starts at slightly more positive potentials. All in all, the ratio of the DES components does not affect the cyclic voltammogram too much. After the addition of Cu(I) or Cu(II) salt (20 mM), the electrolytes are supposed to be stable in the potential window under investigation.

Next, CuCl was added to both ChCl/EG mixtures to perform cyclic voltammetry (Figure 5b). To avoid the formation of Cu^{2+}, a positive potential limit of 0.5 V$_{Cu}$ was chosen. The cyclic voltammograms exhibit a similar shape, but different current densities. At potentials below 0 V$_{Cu}$, bulk deposition takes place.

ChemElectroChem

Articles
doi.org/10.1002/celc.202101283

**Chemistry
Europe**
European Chemical
Societies Publishing

As bivalent Cu^{2+} ions are absent in the electrolyte, copper can only be deposited by a one-electron reduction. In both cases, the charge density for dissolution has almost the same absolute value as that for deposition. Charge densities of $-9870\ \mu C\,cm^{-2}$ and $9860\ \mu C\,cm^{-2}$ were determined for the 16:84 mixture (Figure 5b, shown in blue) and $-5640\ \mu C\,cm^{-2}$ and $5620\ \mu C\,cm^{-2}$ for the 33:67 mixture (Figure 5b, depicted in red). Firstly, this means that copper is dissolved to Cu^+ and not to Cu^{2+}. Secondly, the copper deposition from this DES on Au(111) has a high coulombic efficiency (99.9% and 99.7%).

In the case of the 16:84 mixture with CuCl, the bulk deposition starts at $-0.07\ V_{Cu}$ for a scan rate of $50\ mV\,s^{-1}$. The current density decreases exponentially at the very beginning, as expected from Butler-Volmer kinetics with the electron transfer being the rate-determining step. If the potential is lowered further, the diffusion rate becomes increasingly important, as can be seen from the decreasing slope of the curve. At the minimum of the curve itself, copper deposition is diffusion-controlled. The deposition from the 33:67 mixture exhibits a slightly higher overpotential and the current drops less steeply. This may be related to slightly differing solvation energies of the Cu^+ species, leading to different reorganization energies during the electron transfer and different electro-crystallization kinetics. Additionally, the absolute peak current densities at $-0.2\ V_{Cu}$ in the ChCl/EG 16:84 DES are higher. For the deposition peak around $-0.2\ V_{Cu}$, they differ by a factor of 2.3 compared to the 33:67 electrolyte. It will be demonstrated below that the diffusion coefficients of Cu^+ in these electrolytes differ by a very similar factor (2.4).

If using $CuCl_2$ instead, the cyclic voltammograms are performed with a more positive potential limit (Figure 5c). Around $0.7\ V_{Cu}$, the Cu^+/Cu^{2+} electron transfer redox reaction can be observed, followed by gold surface oxidation positive of $0.9\ V_{Cu}$ which is induced by the high chloride concentration. During the negative-going sweep, the cathodic current reaches zero slowly, implying that Cu^{2+} is steadily reduced to Cu^+ in this potential range. There is a significant difference in the bulk deposition negative of $0\ V_{Cu}$ in the cyclic voltammograms caused by the different molar ratios of ChCl and EG. The deposition and dissolution with ChCl/EG (16:84)$+CuCl_2$ (Figure 5c in blue) resemble the one with CuCl (Figure 5b in blue). This implies that previously reduced Cu^+ is deposited by a one-electron reaction to copper. The coulombic efficiency is again high ($-7290\ \mu C\,cm^{-2}$ and $7220\ \mu C\,cm^{-2}$, *i.e.* 99%). The charge is lower compared to the direct use of CuCl (Figure 5b in blue) because Cu^+ generated *in-situ* is a minority species of low concentration. This leads to less deposition and dissolution.

Interestingly, this cyclic voltammogram of ChCl/EG (16:84)$+CuCl_2$ (Figure 5c in blue) is similar to the one in ChCl/TFA (31:69)$+CuCl_2$ (Figure 8b in red). These two electrolytes are prepared in their particular eutectic ratio. Although the components and ratio differ, the deposition mechanism, *i.e.* that first Cu^{2+} is reduced to Cu^+ and at more negative potentials Cu^+ is reduced to Cu, is comparable. This behavior is known for Cu deposition from aqueous as well as non-aqueous systems[16,17,21] and is attributed to the stabilization of Cu^+ by

chloride.[39] Therefore, a similar stabilization of the Cu^+ species by chloride is assumed to occur in the EG- and TFA-based DESs.

For the ChCl/urea DES, hydrogen bonding between the chloride anion and the HBD is known from theoretical calculations.[40,41] Accordingly, we suspect for the pure DESs (ChCl/EG (16:84) and ChCl/TFA (31:69)) the formation of a weak complex of chloride ions with the respective HBD which is surrounded by choline cations. If the chloride concentration is higher, for example in the ChCl/EG 33:67 DES, chloride is present in excess, and only less chloride could be complexed by the HBD. Higher chloride concentrations stabilize Cu^+, mostly via the formation of $CuCl_2^-$. Cu^{2+} is stabilized as well, but to a lesser extent than Cu^+.[39] During deposition, before copper can crystallize on the electrode, decomplexation of the copper ions has to occur. If the complex is more stable, a higher activation energy, *i.e.* a higher overpotential, is required. According to Sebastián *et al.*, who compared copper electrodeposition from a chloride-containing aqueous electrolyte with a ChCl/urea DES, the deposition is also slower in chloride excess due to Cu^+ stabilization by chloride complexation.[21] The same behavior can also be observed in the systems examined in this study (Figures 5b and c).

If using ChCl/EG in a ratio of 33:67 with $CuCl_2$ (Figure 5c in red), two deposition processes are observable. The first one at $-0.2\ V_{Cu}$ has a lower current density by a factor of 2.3 compared to the 16:84 mixture with $CuCl_2$ (Figure 5c in blue), which again coincides with the lower diffusion coefficient. The mass transport of the Cu^+ species is limited in the 33:67 electrolyte leading to slower deposition. However, a second deposition process is detected at 200 mV more negative potentials. We assume the one-electron reduction being followed by a two-electron reduction from Cu^{2+} to copper (details will be published elsewhere). By chance, this additional deposition leads to similar dissolution currents as in ChCl/EG (16:84)$+CuCl_2$.

Comparing the UPD in the different electrolytes, there are only minor differences. With $CuCl_2$, the first stages of the UPD in the 33:67 mixture are probably already occurring at $0.6\ V_{Cu}$ (Figure S4a). However, these features are hardly recognizable in the 16:84 mixture because they are overlaid by the redox reaction. Due to the lower chloride content, the redox reaction occurs at a lower potential and has a higher current density, therefore masking the UPD. The position of these first UPD peaks can be estimated in Figure 6a. If using CuCl instead, again the first part of the UPD cannot be separated from the redox process. The completion of the first monolayer during the second part of the UPD (Figures 5b and c, S3) is indicated by a peak at $0.05\ V_{Cu}$ which is less sharp compared to the ChCl/EG 33:67 DES. As the latter exhibits a higher chloride concentration, these results suggest that the UPD is strongly influenced by chloride. It is known for aqueous systems that chloride adsorbs on Cu atoms deposited on an Au(111) surface.[19,42,43] Presumably, also in the non-aqueous DESs the copper monolayer is stabilized by adsorbed chloride ions.

To get a better understanding of the diffusion processes of the different copper species, diffusion coefficients were determined. For this purpose, cyclic voltammograms of Au(111) in
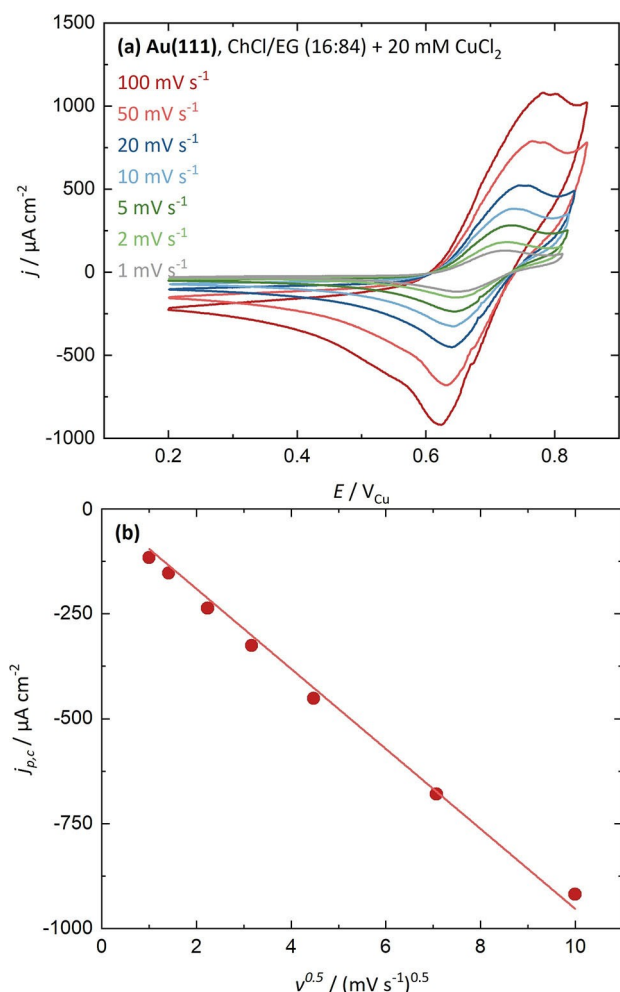
ChemElectroChem

Articles
doi.org/10.1002/celc.202101283

**Chemistry
Europe**
European Chemical
Societies Publishing

Figure 6. a) Cyclic voltammograms at different scan rates of Au(111) in ChCl/EG (16:84) with 20 mM CuCl$_2$. b) Corresponding plot of the cathodic peak current densities *vs.* square root of the scan rate with the corresponding linear fit. A diffusion constant of $3.1 \cdot 10^{-7}$ cm^2 s^{-1} is obtained.

contact with the Cu-containing DES were recorded in a potential range between 0.2 and 0.85 V$_{Cu}$ at different scan rates (Figures 6a, S4a–6a). For the CuCl$_2$-based electrolytes, the cathodic peak current densities are plotted versus the square root of the scan rate (Figures 6b, S4b). The resulting straight line supports the electron transfer between the electrode and the dissolved species (Cu^{2+}). The diffusion coefficients of Cu^{2+}, calculated employing linear regression and the Randles-Sevcik equation (Equation 1), are shown in Table 1. Here, j_p is the peak current density, z the number of transferred electrons, F the Faraday constant, c the concentration, v the scan rate, D the

diffusion coefficient, R the gas constant, and T the temperature. The diffusion coefficients of Cu$^+$ were determined accordingly, except that the anodic instead of the cathodic peak current densities were analyzed (Figures S5b, S6b, Table 1).

$$j_p = 0.4463 \, zFc \sqrt{\frac{zFvD}{RT}} \tag{1}$$

It can be noticed for both ChCl/EG mixtures that the diffusion coefficient of Cu$^+$ is about twice as high as that of Cu^{2+}. Based on the Stokes-Einstein equation (Equation 2) with the dynamic viscosity of the solvent η, conclusions can be drawn about the hydrodynamic radius R_0. If the diffusion coefficient is twice as high, the hydrodynamic radius of Cu$^+$ is only about half that of Cu^{2+}.

$$D = \frac{k_B T}{6\pi \eta R_0} \tag{2}$$

Comparing the diffusion coefficients in the ChCl/EG 16:84 to the 33:67 mixtures, the diffusion is 2.4 times faster in the eutectic 16:84 mixture. This applies to both Cu$^+$ and Cu^{2+} and, as already mentioned, matches very well with the – by a factor of 2.3 – differing peak current densities (Figures 5b and c). That difference can be attributed to the difference in viscosity. It is known that the viscosity decreases with increasing content of ethylene glycol.[30,44] ChCl/EG in a ratio of 33:67 has a viscosity of 48.59 mPa s, whereas for the 17:83 mixture a viscosity of 23.36 mPa s at 298.15 K was found.[44] These values for ratios similar to those investigated in this study differ by a factor of 2.1, which is comparable to the differences we found in electrochemical behavior. This trend can be understood with the Stokes-Einstein equation (Equation 2) since the viscosity is inversely proportional to the diffusion coefficient. Thus, the obtained diffusion coefficients support the results on copper deposition previously discussed and are in good agreement with each other and with the literature.[23]

A diffusion coefficient has also been determined for the ChCl/TFA eutectic (31:69) with CuCl$_2$ (Figure S7). The diffusion is with $9 \cdot 10^{-8}$ cm^2 s^{-1} by a factor of 1.4 lower than in the corresponding ChCl/EG DES. Again, this can be attributed to the different viscosity of the DESs. The viscosity of ChCl/TFA is significantly higher than that of ChCl/EG. For example, the 33:67 (ChCl/TFA) mixture has a viscosity of around 195 mPa s at 298.15 K.[30]

Electrochemical characterization of Au(111) in ChCl/TFA

Likewise, copper deposition onto Au(111) from CuCl- and CuCl$_2$-containing electrolytes was investigated with the ChCl/TFA DES. The selected molar ratios of choline chloride to HBD are the eutectic ratio (31:69), which is compared to one mixture containing more (40:60) and one containing less (20:80) chloride. The measurements are performed at 60 °C to ensure that all mixtures are liquid. Since the densities are not known for all mixtures and two of those are solid at room temperature,

Table 1. Diffusion coefficients of Cu$^+$ and Cu^{2+} in different DESs. Values are given in cm^2 s^{-1}.

	Cu^{2+}	Cu$^+$
ChCl/EG (33:67)	$1.3 \cdot 10^{-7}$ $(1.45–1.6 \cdot 10^{-7})$[23]	$2.8 \cdot 10^{-7}$ $(2.6–2.8 \cdot 10^{-7})$[23]
ChCl/EG (16:84)	$3.1 \cdot 10^{-7}$	$6.7 \cdot 10^{-7}$
ChCl/TFA (31:69)	$9 \cdot 10^{-8}$	

ChemElectroChem

Articles
doi.org/10.1002/celc.202101283

Chemistry Europe
European Chemical
Societies Publishing

a copper concentration of 15 mmol kg^{-1} is used. This corresponds to a concentration of about 20 mmol L^{-1} in the eutectic 31:69 mixture.

First, the underpotential deposition of Cu onto Au(111) is discussed. Cyclic voltammograms for Au(111) in mixtures of ChCl/TFA and CuCl or CuCl$_2$ are shown in Figure 7. The UPD of copper on Au(111) not only proceeds in two steps with EG, as discussed above, but also with TFA as HBD. The same behavior was also observed with urea[22]. Therefore, the initial stages of Cu UPD on Au(111) are expected around 0.6 V$_{Cu}$, followed by the completion of the first monolayer 500 mV more negative. The peaks are less sharp compared to urea or EG, although TFA can be purified thoroughly by sublimation. The transferred charges (-170 to $-200\ \mu C\ cm^{-2}$; 160 to 190 $\mu C\ cm^{-2}$) correspond to the deposition and dissolution of one monolayer, for which 222 $\mu C\ cm^{-2}$ are theoretically expected without anion and capacitive effects. Since the chloride content in the 40:60 mixture is higher and the associated charges are lower, co-adsorption of chloride seems to be important. The beginning of the UPD around 0.6 V$_{Cu}$, which consists of at least two processes, comprises around 60% of the total charge. In the eutectic mixture with CuCl (Figure 7 in red), the oxidation to Cu^{2+} starts more negative than in the 40:60 mixture (Figure 7 in blue). The same has also been observed with EG and is due to the different chloride content. As a result, the first stages of the UPD in the eutectic mixture are more difficult to detect and partially overlaid by oxidation. During the second part around 0.1 V$_{Cu}$, around a third of a monolayer is deposited. The transferred charge is 40% of the total charge with three deposition and at least two dissolution peaks. Different chloride concentrations do not lead to a significant change in the position and shape of the peaks. To elucidate the UPD further, the ChCl/TFA (40:60) DES with CuCl was analyzed by cyclic voltammetry with different scan rates (Figure S8). A linear correlation of maximum current density and scan rate was
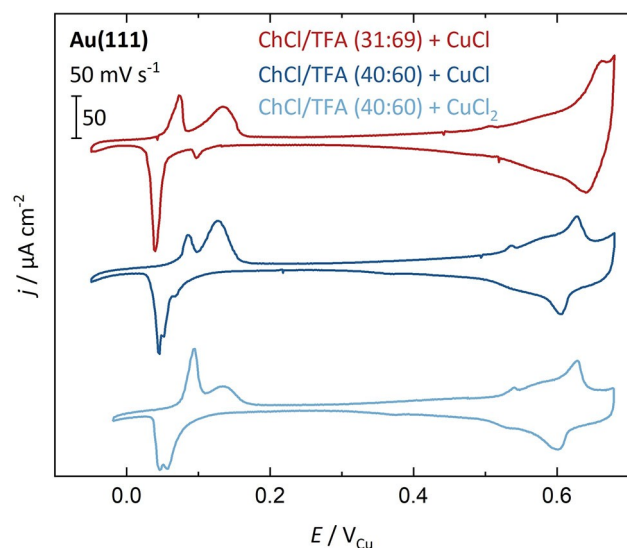
found for all main processes (marked with a black dot). The deposition reaction takes place via a heterogeneous electron transfer with the analyte adsorbing previously on the electrode.

With CuCl$_2$ (Figure 7 in light blue) instead of CuCl (Figure 7 in blue), the basic form is the same and the charges are similar. This again supports the assumption of a one-electron reaction of previously reduced Cu$^+$ to Cu. Otherwise, we would expect twice the charge for a two-electron reduction. The exact processes that take place during the UPD are not yet known. For further clarification, an in-situ STM study would be helpful, but this is beyond the scope of this work. After the UPD (Figure S9), bulk deposition begins with an overpotential of 60 mV versus the copper reference electrode. The dissolution of bulk Cu is separated from the dissolution of the UPD layer, which of course is more stable.

Next, the bulk deposition is investigated from the TFA-based electrolytes. The behavior of Au(111) in CuCl-containing DESs is first studied by cyclic voltammetry (Figure 8a). The dominating deposition reaction is a one-electron reaction of Cu$^+$ to Cu. As with EG as HBD, the maximum current densities of deposition and dissolution depend on the viscosity of the electrolyte. This in turn depends on the composition. At 298.15 K, ChCl/TFA 40:60 exhibits a considerably higher viscosity (257 mPa s) than the 33:67 mixture (195 mPa s).[30] This
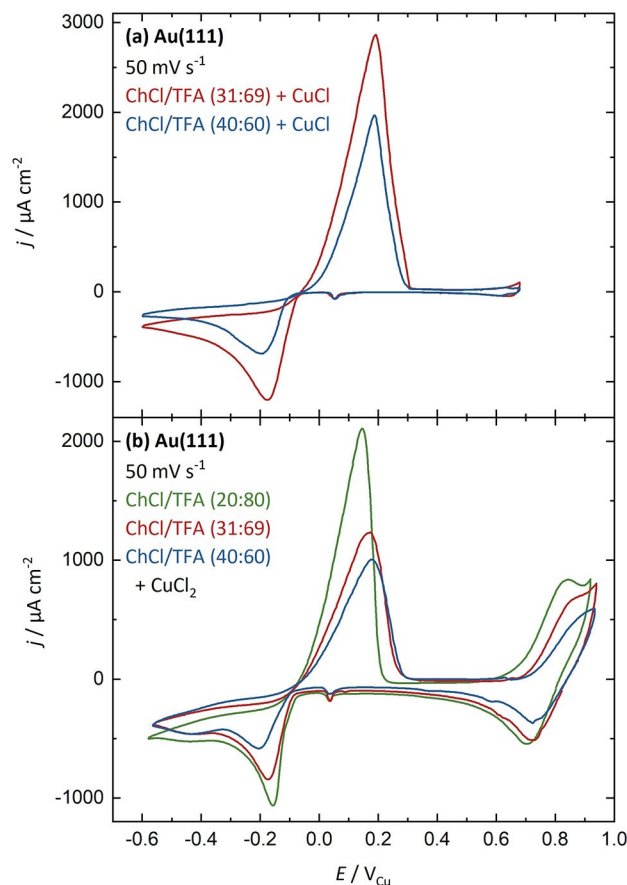

Figure 7. Cyclic voltammograms of Au(111) in ChCl/TFA mixtures in ratios of 31:69 with 15 mmol kg^{-1} CuCl (red), 40:60 with 15 mmol kg^{-1} CuCl (blue) and 40:60 with 15 mmol kg^{-1} CuCl$_2$ (light blue) at a scan rate of 50 mV s^{-1}.

Figure 8. Cyclic voltammograms of Au(111) in ChCl/TFA (20:80 in green, 31:69 in red, and 40:60 in blue) with (a) 15 mmol kg^{-1} CuCl or (b) with 15 mmol kg^{-1} CuCl$_2$ at a scan rate of 50 mV s^{-1}.

ChemElectroChem

Articles
doi.org/10.1002/celc.202101283

**Chemistry
Europe**
European Chemical
Societies Publishing

trend, that the viscosity is lower for higher concentrations of TFA, is also valid for mixtures in other ratios. Therefore, it can be concluded that the viscosity in the eutectic mixture (31:69 in red) is lower than in the 40:60 mixture. Thus, diffusion is faster, and the maximum currents are higher than in the case of excess ChCl (40:60 in blue). The higher currents also lead to higher charges during deposition and dissolution ($-9470\,\mu C\,cm^{-2}$ and $9450\,\mu C\,cm^{-2}$ for 31:69 and $-5610\,\mu C\,cm^{-2}$ and $5560\,\mu C\,cm^{-2}$ for 40:60). In both cases, the reactions exhibit high coulombic efficiencies. However, diffusion should only influence larger currents and not affect the beginning of deposition and dissolution. The differences here can be attributed to different reorganization energies during the electron transfer, also resulting in different exchange current densities. Altogether, despite the different temperatures, there are no major differences in the cyclic voltammograms of bulk deposition with EG compared to TFA as hydrogen bond donor.

With CuCl$_2$, the electrolytes with TFA (Figure 8b) also behave electrochemically similar to those with EG. The ChCl/TFA (20:80) mixture contains the fewest chloride, and we expect the chloride to be again weakly complexed by the HBD, namely the TFA. The deposition (Figure 8b in green) takes place in one step from previously reduced Cu$^+$ to Cu. The eutectic electrolyte (ChCl/TFA 31:69, Figure 8b in red) shows lower currents because of its higher choline chloride content and higher viscosity, as discussed above. Still, the reduction of Cu$^+$ to Cu is the main deposition mechanism, although one can distinguish a second deposition process at $-0.43\,V_{Cu}$. With EG, this has been attributed to a two-electron reduction of Cu^{2+} to Cu and we suspect the same behavior in this case. With a chloride excess in the electrolyte (ChCl/TFA 40:60, Figure 8b in blue), not all chloride can be complexed by TFA. This promotes the second deposition process, which is the reason for its higher peak current density compared to the first. We believe that a complex of Cu^{2+} and chloride is forming, which diffuses faster or is deposited more easily. Comparing successively recorded cycles (Figure S10), the second deposition peak becomes progressively smaller, and less Cu^{2+} is reduced. Probably the deposition via Cu$^+$ is more efficient, as only one electron has to be transferred during the reaction.

With higher chloride concentration, the total charge during deposition and dissolution as well as the reversibility decrease. As discussed for CuCl, with increasing viscosity the charge of Faraday processes such as metal deposition decreases. The reversibility decreases because of the second deposition process occurring to a greater extent. This reaction consumes two electrons for one Cu atom to be deposited but releases only one electron during dissolution. Moreover, the Cu$^+$/Cu^{2+} redox reaction is shifted to more positive potentials with a higher chloride concentration (Figure 8b).

Comparing the CuCl$_2$-containing ChCl/TFA and ChCl/EG DESs in their eutectic ratio, the influence of the chloride concentration is smaller with TFA, as described above. Using EG, the second deposition process exhibits a higher peak current density than the first, whereas with TFA still the first peak corresponds to the main deposition reaction. It could be assumed that this is due to the different hydrogen bond donors EG and TFA complexing the chloride ions to a different extent. If less chloride is complexed by the HBD, the free chloride concentration is higher – as observed for the higher choline chloride content – and the second deposition process prevails. Following this reasoning, complexation of chloride by EG is weaker than with TFA. This hypothesis is supported by the fact that hydroxyl groups are weaker hydrogen bond donors than amino groups[45] and TFA is presumably linked to chloride by its amino group whereas EG is linked by its hydroxyl group. It can be concluded that by choosing the hydrogen bond donor and its molar ratio to the choline salt, the deposition behavior can be controlled depending on the application.

In our understanding, DESs are non-aqueous electrolytes with a high concentration of ions provoking their properties. The characteristics are not caused by freezing-point depression at the eutectic point but are tunable by composition. It seems that the intermolecular interactions and the coordination of the choline counter ion to the hydrogen bond donor are the more important parameters for the electrochemical behavior.

Conclusion

First, phase diagrams were composed for two different DESs based on choline chloride as organic salt. The hydrogen bond donors used are ethylene glycol and trifluoroacetamide. The eutectic ratio of the well-known choline chloride/ethylene glycol DES is 16:84, in contrast to the most commonly used mixture with a ratio of 33:67. The eutectic temperature is $-27.6\,°C$. For the choline chloride/trifluoroacetamide DES, a ratio of 31:69 was determined with a eutectic temperature of $12.5\,°C$. These results demonstrate that the nature of the hydrogen bond donor is crucial for the thermal properties, *i.e.* for the eutectic ratio as well as the eutectic temperature.

Secondly, the electrodeposition of copper onto Au(111) from these electrolytes was studied in detail by cyclic voltammetry. The influence of the hydrogen bond donor and the composition, *i.e.* the ratio of choline chloride to the hydrogen bond donor was investigated. The latter does not affect the deposition mechanism in terms of the reactions taking place if using CuCl as a copper source. The UPD on Au(111) is followed by bulk deposition, whereby the transferred charge depends on the diffusion rate of Cu$^+$. The Cu$^+$ species diffuse faster in electrolytes with lower viscosity, and the viscosity can be tuned by varying the composition. With CuCl$_2$ as a copper source, also Cu^{2+} is deposited in a two-electron reaction about 200 mV more negative than the deposition via Cu$^+$. To which extent this reaction takes place, depends on the composition: The more choline chloride is present in the electrolyte, the more predominates the deposition of Cu^{2+}. Also, this phenomenon is influenced by the hydrogen bond donor. For similar mixing ratios of choline chloride to hydrogen bond donor, the deposition via Cu^{2+} occurs to a lesser extent if trifluoroacetamide is involved. We ascribe this to the nature of the hydrogen bond donor, as trifluoroacetamide can complex

ChemElectroChem

Articles
doi.org/10.1002/celc.202101283

Chemistry
Europe
European Chemical
Societies Publishing

the chloride ions stronger to its amino group by hydrogen bonds, than the ethylene glycol to its hydroxyl group.

Our study suggests, however, that it is not important for the electrodeposition of copper on Au(111) whether the DES electrolyte is present in the eutectic ratio. Instead, the composition and choice of components can be employed to control the properties of the electrodeposition. This underlines that deep eutectic solvents can be widely applied as versatile and adaptable non-aqueous electrolytes.

Experimental Section

The DESs were prepared according to the ratios given in the text by mixing a choline salt, an HBD, and if required, a copper salt under N_2 atmosphere ($H_2O < 0.5$ ppm, $O_2 < 0.5$ ppm) in a glovebox (MBraun). The mixtures were stirred at room temperature or heated up to 60 °C until homogeneous liquids were obtained. Choline chloride (Alfa Aesar, 98 + %) was recrystallized twice from absolute ethanol (Merck, 99.9 %). Ethylene glycol (Sigma Aldrich, 99.8 %) was used as received and trifluoroacetamide (Sigma Aldrich, 97 %) was purified by sublimation at 60 °C. Copper(II) chloride dihydrate (Merck, 99 + %) was dehydrated under vacuum before usage, whereas copper(I) chloride (Sigma Aldrich, 99.995 + %) was used as received.

DSC measurements were carried out with a DSC250 from TA Instruments with liquid nitrogen cooling. The calibration of the DSC was conducted so that the temperature deviation was below 0.2 °C and the deviation in enthalpy less than 1 %. The samples (5–10 mg) were placed in Tzero aluminum pans from TA Instruments with a normal and a hermetic lid and hermetically sealed in the glovebox to prevent ingress of water and oxygen. The DSC cell was purged with helium (25 mL min^{-1}) during the measurements. The samples were cooled down in a controlled manner (10 °C min^{-1}) from 80 °C to −100 °C and subsequently heated slowly (0.2 °C min^{-1}) to 100 °C. Between each of these steps, the temperature was held isothermally for 5 minutes. Only the heating step for each sample is presented here, as only the melting and not the crystallization is of interest. The very slow heating rate is chosen to separate the recrystallization and the two melting peaks from each other, to determine a more accurate heating enthalpy by integration. For evaluation, the TRIOS software from TA Instruments was used.

The cyclic voltammetry was carried out with a Zahner IM6 Potentiostat from Zahner Elektrik in the before mentioned glovebox using a cell with a volume of 0.25 cm^3 made of Kel-F™. As a working electrode, an Au(111) single crystal of 12 mm diameter (MaTecK GmbH, Jülich, Germany) and as counter and reference electrodes, a Pt, respectively Cu wire was used.

Conflict of Interest

The authors declare no conflict of interest.

[1] K. Xu, *Chem. Rev.* **2004**, *104*, 4303–4418.
[2] R. Mohtadi, F. Mizuno, *Beilstein J. Nanotechnol.* **2014**, *5*, 1291–1311.
[3] A. Ponrouch, D. Monti, A. Boschin, B. Steen, P. Johansson, M. R. Palacín, *J. Mater. Chem. A* **2015**, *3*, 22–42.
[4] W. Simka, D. Puszczyk, G. Nawrat, *Electrochim. Acta* **2009**, *54*, 5307–5319.
[5] F. Endres, *ChemPhysChem* **2002**, *3*, 144–154.
[6] F. Liu, Y. Deng, X. Han, W. Hu, C. Zhong, *J. Alloys Compd.* **2016**, *654*, 163–170.
[7] S. Survilienė, S. Eugénio, R. Vilar, *J. Appl. Electrochem.* **2011**, *41*, 107–114.
[8] Z. W. Seh, J. Sun, Y. Sun, Y. Cui, *ACS Cent. Sci.* **2015**, *1*, 449–455.
[9] H. Royle, *Environ. Res.* **1975**, *10*, 39–53.
[10] Y. Sheasha, D. Yücel, L. A. Kibler, M. Knape, S. Holl, S. Henne, S. Heitmüller, T. Jacob, *ChemElectroChem* **2017**, *4*, 1390–1394.
[11] A. P. Abbott, G. Capper, D. L. Davies, R. K. Rasheed, V. Tambyrajah, *Chem. Commun.* **2003**, *8*, 70–71.
[12] A. P. Abbott, J. C. Barron, K. S. Ryder, D. Wilson, *Chem. Eur. J.* **2007**, *13*, 6495–6501.
[13] E. L. Smith, A. P. Abbott, K. S. Ryder, *Chem. Rev.* **2014**, *114*, 11060–11082.
[14] D. Carriazo, M. C. Serrano, M. C. Gutiérrez, M. L. Ferrer, F. del Monte, *Chem. Soc. Rev.* **2012**, *41*, 4996–5014.
[15] M. U. Ceblin, S. Zeller, B. Schick, L. A. Kibler, T. Jacob, *ChemElectroChem* **2019**, *6*, 141–146.
[16] A. P. Abbott, K. El Ttaib, G. Frisch, K. J. McKenzie, K. S. Ryder, *Phys. Chem. Chem. Phys.* **2009**, *11*, 4269–4277.
[17] P. Sebastián, E. Vallés, E. Gómez, *Electrochim. Acta* **2014**, *123*, 285–295.
[18] N. Batina, T. Will, D. Kolb, *Faraday Discuss.* **1992**, *94*, 93–106.
[19] E. Herrero, L. J. Buller, H. D. Abruña, *Chem. Rev.* **2001**, *101*, 1897–1930.
[20] F. Endres, A. Schweizer, *Phys. Chem. Chem. Phys.* **2000**, *2*, 5455–5462.
[21] P. Sebastián, E. Torralba, E. Vallés, A. Molina, E. Gómez, *Electrochim. Acta* **2015**, *164*, 187–195.
[22] P. Sebastián, E. Gómez, V. Climent, J. M. Feliu, *Electrochem. Commun.* **2017**, *78*, 51–55.
[23] D. Lloyd, T. Vainikka, L. Murtomäki, K. Kontturi, E. Ahlberg, *Electrochim. Acta* **2011**, *56*, 4942–4948.
[24] D. Shen, K. Steinberg, R. Akolkar, *J. Electrochem. Soc.* **2018**, *165*, E808-E815.
[25] Y. Su, J. Liu, R. Wang, S. Aisa, X. Cao, S. Li, B. Wang, Q. Zhou, *J. Electrochem. Soc.* **2018**, *165*, H78-H83.
[26] H. G. Morrison, C. C. Sun, S. Neervannan, *Int. J. Pharm.* **2009**, *378*, 136–139.
[27] M. Gilmore, M. Swadzba-Kwasny, J. D. Holbrey, *J. Chem. Eng. Data* **2019**, *64*, 5248–5255.
[28] R. L. Collin, *J. Am. Chem. Soc.* **1957**, *79*, 6086.
[29] G. W. H. Höhne, W. F. Hemminger, H.-J. Flammersheim, *Differential Scanning Calorimetry*, Springer, Berlin/Heidelberg **2003**.
[30] K. Shahbaz, F. S. Mjalli, M. A. Hashim, I. M. ALNashef, *J. Appl. Sci.* **2010**, *10*, 3349–3354.
[31] A. P. Abbott, G. Capper, B. G. Swain, D. A. Wheeler, *Trans. IMF* **2005**, *83*, 51–53.
[32] A. P. Abbott, G. Capper, D. L. Davies, K. J. McKenzie, S. U. Obi, *J. Chem. Eng. Data* **2006**, *51*, 1280–1282.
[33] A. P. Abbott, R. C. Harris, K. S. Ryder, *J. Phys. Chem. B* **2007**, *111*, 4910–4913.
[34] F. G. Bagh, K. Shahbaz, F. S. Mjalli, I. M. AlNashef, M. A. Hashim, *Fluid Phase Equilib.* **2013**, *356*, 30–37.
[35] L. P. Silva, M. A. R. Martins, J. H. F. Conceição, S. P. Pinho, J. A. P. Coutinho, *ACS Sustainable Chem. Eng.* **2020**, *8*, 15317–15326.
[36] Z. Wang, T. Wu, X. Geng, J. Ru, Y. Hua, J. Bu, Y. Xue, D. Wang, *J. Mol. Liq.* **2022**, *346*, 117059.
[37] X. Meng, K. Ballerat-Busserolles, P. Husson, J.-M. Andanson, *New J. Chem.* **2016**, *40*, 4492–4499.
[38] A. van den Bruinhorst, L. J. B. M. Kollau, M. C. Kroon, J. Meuldijk, R. Tuinier, A. C. C. Esteves, *J. Chem. Phys.* **2018**, *149*, 224505.

ChemElectroChem

Articles
doi.org/10.1002/celc.202101283

Chemistry Europe
European Chemical
Societies Publishing

[39] H. Zhao, J. Chang, A. Boika, A. J. Bard, *Anal. Chem.* **2013**, *85*, 7696–7703.
[40] H. Sun, Y. Li, X. Wu, G. Li, *J. Mol. Model.* **2013**, *19*, 2433–2441.
[41] S. Zahn, B. Kirchner, D. Mollenhauer, *ChemPhysChem* **2016**, *17*, 3354–3358.
[42] Z. Shi, S. Wu, J. Lipkowski, *Electrochim. Acta* **1995**, *40*, 9–15.
[43] Z. Shi, S. Wu, J. Lipkowski, *J. Electroanal. Chem.* **1995**, *384*, 171–177.
[44] N. F. Gajardo-Parra, V. P. Cotroneo-Figueroa, P. Aravena, V. Vesovic, R. I. Canales, *J. Chem. Eng. Data* **2020**, *65*, 5581–5592.

[45] J. Hladílková, H. E. Fischer, P. Jungwirth, P. E. Mason, *J. Phys. Chem. B* **2015**, *119*, 6357–6365.

ARTICLES

Diving into Deep Eutectic Solvents: Having identified the eutectic ratio and temperature of two Deep Eutectic Solvents (DESs) type III, Cu electrodeposition on Au(111) from those DESs in different molar ratios was studied. The deposition mechanism is explained by the high ion concentration rather than the thermal properties of DESs. With more Cl^- present and depending on the hydrogen bond donor, the diffusion rate of Cu species changes, and not only Cu^+ but also Cu^{2+} is reduced.
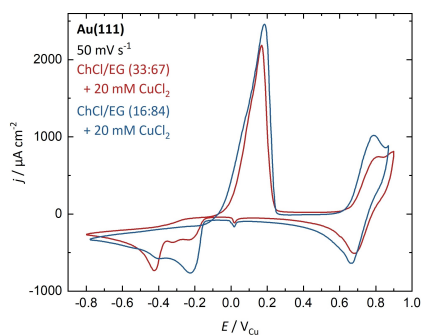
T. Geng, S. J. Zeller, Dr. L. A. Kibler, Dr. M. U. Ceblin*, Prof. Dr. T. Jacob*

1 – 12

Electrodeposition of Cu onto Au(111) from Deep Eutectic Solvents: Molar Ratio of Salt and Hydrogen Bond Donor